J. Electroanal. Chem., 124 (1981) 73—86
Elsevier Sequoia S.A., Lausanne — Printed in The Netherlands

DIFFUSION PROCESSES AT FINITE (MICRO) DISK ELECTRODES SOLVED BY DIGITAL SIMULATION

JÜRGEN HEINZE

Institut für Physikalische Chemie der Universität Freiburg, Albertstr. 21, D-7800 Freiburg (F.R.G.)

(Received 26th August 1980; in revised form 12th January 1981)

ABSTRACT

A modified simulation model based on a two-dimensional implicit difference approximation (ADI method) has been developed to describe diffusion processes at stationary unshielded (micro) disk electrodes. Besides the semi-infinite linear component, the model also takes into account a radial diffusion gradient which is always present in all transport processes of this nature. The current—time relationship for diffusion-controlled electrolysis was used to test the consistency and accuracy of the numerical approximation. The computation reveals, in close agreement with experimental data, that the familiar Cottrell equation should be replaced by the formula:

$$it^{1/2}/nFAc^{b}D^{1/2} = \pi^{-1/2}\{1 + b(Dt/R^2)^{1/2}\}$$

where the coefficient b, dependent on $(Dt/R^2)^{1/2}$, can take values between 1.772 . . . and 2.257 . . ..

INTRODUCTION

Much research has been done on electrode reactions in which the mass transport of electroactive species takes place almost exclusively by means of diffusion. Although the hanging mercury drop electrode (HMDE) is still employed, in recent years stationary solid electrodes have increasingly been used [1]. In particular, in the analysis of oxidative processes metal electrodes or graphite are indispensable. Of the different types of electrode available, the planar disk electrode has proved particularly effective. The easily reproducible geometry and ease with which the electrode surface can be cleaned have contributed to the increasing popularity of the disk compared to the spherical, wire or capillary electrode. For some years now there has also been a trend to micro disk electrodes. The reason for this may be that only small sample volumes are needed, and that iR drop effects and capacity currents are rather small. Furthermore, the small electroactive area of a micro disk electrode makes it especially suited for measurements in living tissues.

The theoretical treatment of the current at the disk electrode appears simple: proceeding from the model of semi-infinite linear diffusion, one can obtain a closed solution for the transport equation [2]. However, as early as 1902, Cottrell produced measurements which revealed deviations from theoretical

0022-0728/81/0000—0000/$02.50,

predictions; at the time, the cause of edge effects was not known. Consequently, to eliminate the latter, disk electrodes were often shielded in protective tubes [3—5]. However, as the construction, and the elimination of disturbances in such apparatus involved a great deal of effort [6], the edge of the disk was embedded without shielding in glass, ceramic or another material to allow for the full effect of peripheral influences.

The differences between the properties of an ideal plane and a disk of finite size are significant in the case of the diffusion-controlled current and may not be neglected in the evaluation. In addition, one often notices that chronoamperometric i—$t^{1/2}$ data deviate slightly from the theoretical proposed linearity with increasing experimental time. Similar phenomena are also observed in other electroanalytical methods, e.g. cyclic voltammetry [7] or chronopotentiometry [8]. Although these effects may lead to an incorrect interpretation of electrochemical data obtained at disk electrodes, a closed mathematical solution of this diffusion problem is not yet available. At first Bard and Lingane [8,9] calculated the nature and size of corrective terms in the Cottrell and Sand equations. Both authors take the view that the causes of the observed edge effects lie in radial or quasi-spherical diffusion components, as well as in convection influences. A theoretical study by Soos and Lingane [10] shows that the modified Cottrell equation, in the form:

$$\frac{it^{1/2}}{nFAc^{b}D^{1/2}} = \pi^{-1/2}\left(1 + b\left[\frac{Dt}{R^2}\right]^{1/2}\right) \tag{1}$$

provides a satisfactory agreement with the experimental results. The symbols used in eqn. (1) have their customary meanings. The constant b in the correction term was calculated as 2.26. Evaluating results of i—t measurements gave a value of 2.12 ± 0.10. In a further study Flanagan and Marcoux [11] presented a simple simulation model in which they established a constant value for b of 1.92. For medium measuring times and large electrode size this value agrees fairly closely with the experimental data, but it is too small in the case of small electrode size and long electrolysis times. Recently Kakihana et al. [12,13] corrected the model of Flanagan and Marcoux; they calculated the value of the coefficient b as lying between 1.77 and 1.98. Most recently Aoki and Osteryoung [14] have developed a new analytical solution. They give very reasonable results for large and extremely small values of the correction term to the Cottrell equation. The experimentally observed values for b published in the literature [9,12,15—18] are similar to these theoretical predicted results. They range between 1.77 and 3.21, whereby the upper limit is reached only in the case of carbon fiber electrodes and never at polished Pt electrodes.

In analysing transport phenomena at the planar stationary disk electrode one can assume that normally in the presence of a supporting electrolyte only diffusion processes play a role; accordingly, convection and migration may be disregarded. However, in contrast to the ideal infinite plane, an additional radial concentration gradient must be taken into account for the finite disk. Formally, this gradient is superimposed upon the semi-infinite linear diffusion term in all space points. The corresponding partial differential equation is then

$$\frac{\partial c}{\partial t} = D\left[\frac{\partial^2 c}{\partial r^2} + \frac{1}{r}\left(\frac{\partial c}{\partial r}\right) + \frac{\partial^2 c}{\partial z^2}\right]. \tag{2}$$

Thus far, an exact solution of eqn. (2), taking into account the boundary conditions of semi-infinite diffusion to a circular electrode, has not been produced. In particular, for the medium domain of the current function, which is equally important in electroanalytical work, the known corrections to the Cottrell equation are not fully satisfactory. Recently, the concept of digital simulation has been gaining increasing recognition [19,20]. In view of its physical descriptiveness and its very high consistency, it seems an ideal approximation for all problems involving intricate initial and boundary conditions. Therefore, an improved digital simulation model will be presented here, in which the partial differential eqn. (2) will be analyzed on the basis of a two-dimensional implicit difference approximation. Simply by changing the initial and boundary conditions it is possible to apply this model to other problems involving the disk electrode in electroanalytical chemistry.

CONSTRUCTION OF THE MODEL

The principles of the simulation method (finite difference approximation) have been discussed in detail in the literature [20]. Therefore, we shall restrict ourselves to those details indispensable for an understanding of the model.

The transfer and application of one-dimensional formulations to spatial problems causes, in principle, no great difficulty. However, the consistency, convergence and stability of each new method must be carefully tested, especially as, in the lack of an exact solution, these are the only criteria for testing the value of an approximation. For the present model an implicit alternating direction method (ADI) — based on a modified Crank—Nicolson formalism [21—23] — seems the most suitable; this has been confirmed by the author's analysis [24]. In contrast to an explicit technique, whose stability is restricted the ADI method used here is unconditionally stable. Moreover, the truncation error for all increments is of second order, and round-off errors, which often impair the accuracy of such methods, can be disregarded here [25].

The spatial diffusion towards unshielded disk electrodes can be represented as a vectorial addition with two components, directed perpendicularly and radially respectively, to the disk surface in a solution of infinite volume. For this purpose the model is subdivided in the range parallel to the electrode surface into a finite number of thin layers, each with a height Δz. The electrode and its isolating environment form the boundary of the first layer. Each individual layer consists of a cylinder of radius Δr_1 with its axis in the center of the electrode, and a finite series of concentric annular boxes of width Δr. The individual layers, denoted by the index parameter k, are numbered in increasing order from 0. The radial index number j starts with the innermost cylinder, which has the figure 1. In general, the length of the radius Δr_1 of the inner cylinder is the same as the width Δr of the succeeding annuli. For problems involving small radial gradients of diffusion one may save computer time and storage by taking Δr_1 as a multiple of Δr. As an additional subcondition the following relation between the radius r_0 of the electrode and the magnitude Δr_1 and Δr must be fulfilled:

$$r_0 = \Delta r_1 + (n_r - 1)\,\Delta r\,, \tag{3}$$

(n_r = number of the volume elements covering the electrode). In this way one ensures that the outer wall of an annular box is always flush with the edge of the electrode. In the interest of accuracy, the number of elements j covering the electrode in the radical direction should be at least 30.

The volume of the element in the kth layer and in the jth annulus is given by ($\Delta r = \Delta r_1$):

$$V_{j,k} = \Delta z \pi (2j - 1)\, \Delta r^2 \tag{4}$$

The coordinates of the equidistant surface areas of each volume box are not identical with the positions of the points of the concentration values computed from the difference approximation. As a rule these are located at the center of the individual elements (centered grid) and form their own network with mesh distances Δr and Δz. Although, strictly speaking, only discretized states are theoretically possible, if the increments selected are sufficiently small one can assume that the approximated concentration values can be applied as an average to the total volume element.

Taking into account the volume magnitudes, $V_{j,k}$, the amounts of their interfacing areas, $F_{j,k}$, in the direction of flux, and the space—time increments, Δr, Δz and Δt, one can calculate the changes in the concentrations after the time interval $(l + 1)\, \Delta t$, from the known concentrations $c^l_{j,k} = c(j\, \Delta r,\ k\, \Delta z,\ l\, \Delta t)$. To simplify matters, all concentrations used in the simulation are to be treated as dimensionless quantities ($c_{j,k} = c/c^b$, c^b = bulk concentration). First taking the diffusion in the radial direction, by solving the sets of simultaneous equations (5), one obtains the unknowns $c^{l+1/2}_{j,k}$ after the time interval $\Delta t/2$:

$$c^{l+1/2}_{j,k} - c^l_{j,k} = \frac{D\Delta t}{2}\left[\frac{F_{j,k}}{V_{j,k}\, \Delta r}\left(c^{l+1/2}_{j+1,k} - c^{l+1/2}_{j,k}\right) - \frac{F_{j-1,k}}{V_{j,k} \cdot \Delta r}\left(c^{l+1/2}_{j,k} - c^{l+1/2}_{j-1,k}\right)\right.$$

$$\left. + \frac{1}{\Delta z^2}\left(c^l_{j,k+1} - 2c^l_{j,k} + c^l_{j,k-1}\right)\right] \tag{5}$$

$$1 \leqslant j \leqslant J, \qquad (k = 1, 2, \ldots)$$

In the kth layer $F_{j,k}$ is the interfacing area between the $(j + 1)$th and the jth volume element, and $F_{j-1,k}$ the corresponding area between the jth and the $(j - 1)$th element. Rewriting eqn. (5) and substituting the expressions for the areas and volumes gives the following simplified relationship for the radial diffusion in the time interval $\Delta t/2$:

$$c^{l+1/2}_{j,k} - c^l_{j,k} = \frac{\beta}{2}\left[\frac{1}{2j-1}(2jc^{l+1/2}_{j+1,k} - (4j - 2)\, c^{l+1/2}_{j,k} + (2j - 2)\, c^{l+1/2}_{j-1,k})\right.$$

$$\left. + (c^l_{j,k+1} - 2c^l_{j,k} + c^l_{j,k-1})\right] \tag{6a}$$

$$2 \leqslant j \leqslant J, \qquad (k = 1, 2, \ldots), \qquad \Delta r = \Delta z \qquad \beta = \frac{D\, \Delta t}{\Delta r^2}$$

If $j = 1$ the differential equation to be solved has a singularity. The necessary difference formula can be derived from eqn. (5):

$$c^{l+1/2}_{1,k} - c^l_{1,k} = \frac{\beta}{2}\left[\frac{4}{3}\left(c^{l+1/2}_{2,k} - c^{l+1/2}_{1,k}\right) + \ldots\right], \qquad (k = 1, 2, \ldots) \tag{6b}$$

The computation of the changes in the concentration in the normal direction to the electrode area is straightforward as, with the exception of the electrode—electrolyte boundary, the area and volume values remain constant.

$$c_{j,k}^{l+1} - c_{j,k}^{l+1/2} = \frac{\beta}{2}\left[\left(c_{j,k+1}^{l+1} - 2c_{j,k}^{l+1} + c_{j,k-1}^{l+1}\right) + \frac{1}{2j-1}\left(2jc_{j+1,k}^{l+1/2} - (4j-2)\,c_{j,k}^{l+1/2} + (2j-2)\,c_{j-1,k}^{l+1/2}\right)\right] \qquad 1 \leqslant k \leqslant K, \qquad (j = (1), 2, 3, \ldots) \tag{7}$$

A direct connection between the experimental event and the simulation model can be verified with the aid of a few basic parameters. In the present case the dimensionless relation:

$$\left(\frac{Dt}{R^2}\right)^{1/2} = \left(\frac{Dl\,\Delta t}{(n_r\,\Delta r^2)}\right)^{1/2} \equiv \eta \tag{8}$$

(l = number of Δt loops needed to simulate the experimental time t) is both necessary and sufficient for the precise transfer of the experimental conditions of the transport process to the "simulator". Because of the great stability of the implicit formulation the magnitudes D and $r_0 = n_r\,\Delta r$, as well as the increments Δt, Δr and Δz, can, for the most part, be arbitrarily selected. Nevertheless, a maximum value of 20 is appropriate for $\beta = D\,\Delta t/\Delta r^2$ to avoid discretization errors and convergence problems.

INITIAL AND BOUNDARY CONDITIONS

The sets of simultaneous equations, (6) and (7), describe the diffusion in the inner domain of the model. The simulation is carried out under the assumption that a reversible electrochemical reaction:

$$A \pm ne^- \rightarrow B \tag{9}$$

takes place at the disk surface, whereby the chosen potential necessary for the diffusion control must satisfy the limiting current conditions. With the additional assumption of an infinite volume around the disk, the following initial and boundary conditions hold for the normalized concentration function:

$$c(r, 0, t) = \begin{cases} 0, & r \leqslant r_0,\ t \geqslant 0^+ \\ 1, & r > r_0,\ t = 0 \end{cases} \tag{10a}$$

$$\frac{\partial c}{\partial z}(r, 0, t) = 0, \qquad r > r_0,\ t \geqslant 0^+ \tag{10b}$$

$$c(r, z, 0^+) = 1, \qquad z > 0 \tag{10c}$$

$$\lim_{r\to\infty} c(r, z, t) = \lim_{z\to\infty} c(r, z, t) = 1, \qquad t \geqslant 0^+ \tag{10d}$$

As the effects of truncation and discretization errors are strengthened in a two-dimensional difference model, Taylor power series were used to determine the boundary conditions to the second approximation. It follows from Taylor's expansion and the geometry as a whole that the optimal distance in the

z direction between the concentrations $c_{j,0}$ and $c_{j,1}(j = 1, 2, ...)$ must be $\Delta z/2$. Correspondingly, the thicknesses of layer 0 and layer 1 perpendicular to the phase boundary are reduced to $\Delta z/4$ and $3/4\ \Delta z$ respectively. Furthermore, the discretized concentration quantities $c_{j,0}$ and $c_{j,1}$ $(j = 1, 2, ...)$ shift in the case of layer 0 from the centered normal position to the disk surface, and in the case of layer 1 to a distance of $\Delta z/4$ from the lower boundary area. The details of this construction are shown in Fig. 1.

The time-dependent changes in the concentrations in the two layers immediately above the electrode surface can be described by the following difference expression:

$$\frac{\Delta c_{j,k}}{\Delta t} = \frac{D}{\Delta z^2}\frac{4}{3}(c_{j,2} - 3c_{j,1} + 2c_{j,0}); \qquad k = 0, 1; \qquad (j = 1, 2, ...) \tag{11}$$

(For clarity, all formula are given in explicit form.)

In general, the equation:

$$f_{j,0} = \frac{D}{\Delta z}\frac{1}{3}(-c_{j,2} + 9c_{j,1} - 8c_{j,0}), \qquad (j = 1, 2, ...) \tag{12}$$

holds for the fractional flux, stationary in the time interval Δt, across the total phase boundary.

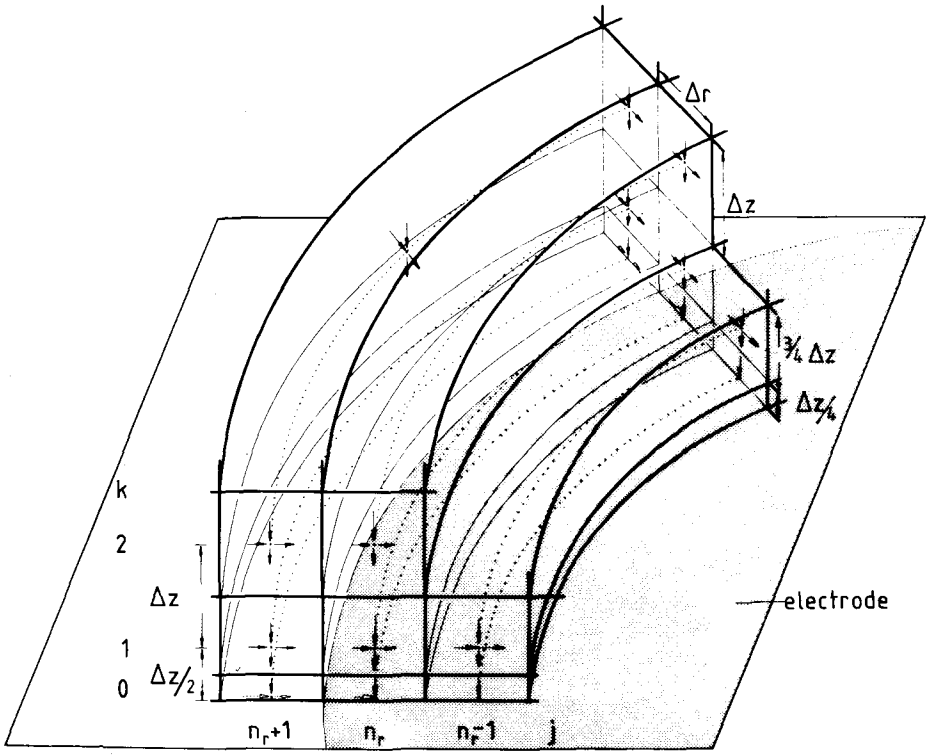

Fig. 1. Structure of the space grid in the region of the electrode interface. k is the number of elements in normal direction to the electrode and n_r the number of the outermost annular element which covers the electrode. (- - - - -) "Lines" at which the concentration values in the individual volume elements are calculated; (——→) direction of flux.

In the boundary region of the disk ($z = 0$, $r \leqslant r_0$; $k = 0$, $j = 1, \ldots, n_r$), the solution of the differential equation is already given (Dirichelet's boundary condition). In accordance with eqn. (10a), the concentration there takes the value 0.

By contrast, for the insulation surfaces outside the disk ($z = 0$, $r > r_0$; $k = 0$, $j > n_r$), only the flux at the phase boundary is known (Neumann's boundary condition). As no particles pass perpendicular to the surface the flux in this direction must equal zero (eqn. 10b). Thus, the different boundary conditions in both regions within and outside the disk produce the following difference equations:

$$\frac{\Delta c_{j,1}}{\Delta t} = \frac{D}{\Delta z^2}\frac{4}{3}(c_{j,2} - 3c_{j,1}) = \frac{D}{\Delta z^2}\left(c_{j,2} - c_{j,1} - \frac{f^z_{j,0}\,\Delta z}{D}\right) \tag{13a}$$

$$f^z_{j,0} = \frac{D}{\Delta z \cdot 3}(9c_{j,1} - c_{j,2}), \qquad (j = 1, 2, \ldots, n_r) \tag{13b}$$

$$\frac{\Delta c_{j,1}}{\Delta t} = \frac{D}{\Delta z^2}(c_{j,2} - 3c_{j,1} + 2c_{j,0}) \tag{14a}$$

$$\frac{\Delta c_{j,0}}{\Delta t} = \frac{D}{\Delta z^2}\,8(c_{j,1} - c_{j,0}) \tag{14b}$$

$$f^z_{j,0} = 0, \qquad (j > n_r) \tag{14c}$$

With the exception of layer 0, the radial diffusion is not subject to any restrictions. The radial flux disappears only in the boundary layer in the region of the disk, which must be treated as an equipotential area. Hence, its gradient outside the electroactive area may extend only to the edge of the disk.

As, in accordance with eqn. (10a), the stationary concentration must also be zero in the outermost volume box of the disk surface ($j = n_r$; $k = 0$), the difference equation for the radial change in the concentration in the first element just outside the electrode ($j = n_r + 1$, $k = 0$) takes the following form:

$$\frac{\Delta c_{n_r+1,0}}{\Delta t} = \frac{D}{\Delta r^2(2n_r + 1)}[2(n_r + 1)\,c_{n_r+2} - (4n_r + 2)\,c_{n_r+1}] \tag{15a}$$

The corresponding radial flux, superimposed upon the normal component in the outer element n_r of the electrode, is given by

$$f^r_{n_r,0} = \frac{D}{\Delta r}\,c_{n_r+1} \tag{15b}$$

In Fig. 1 the possible flux directions in the region at and above the electrode surface are indicated by arrows.

If the mesh size of the network is too large the model computation shows that the radial diffusion in layer 0 produces too large a flux quantity in the outer element n_r of the disk. The opposite effect occurs if the total radial diffusion in layer 0 ($k = 0$) is not taken into account. As in this case it is not necessary to determine directly the concentration c_0 in the boundary annuli of

layer 0 outside the electrode, eqns. (14b) and (15) do not apply and eqn. (14a) is simplified.

$$\frac{\Delta c_{j,1}}{\Delta t} = \frac{D}{\Delta z^2}(c_{j,2} - c_{j,1}) , \qquad (j > n_r, k = 1) . \tag{16}$$

The comprehensive model computations show that the second approximation usually takes less time and, as a rule, converges more quickly than the first solution. Accordingly, the results presented in the next section are based for the most part on the second variant.

Equation (13b) describes the fractional flux through a surface element j of the disk with a base area

$$a_j = \pi \, \Delta r^2 (2j - 1) \tag{17}$$

This flux, multiplied by the concentration of the original species, gives the mole number which in the square unit diffuses to the disk surface in Δt s.

$$\phi_j^z = f_{j,0}^z \, c \tag{18}$$

It is directly proportional to the electron flux or the current, as the case may be, in the surface segment concerned. As the fractional fluxes must be weighted in accordance with their area size to determine the total flux through the electrode, one normalizes the individual surface increments a_j in relation to total electrode area A. This gives the following expression for the real individual current densities:

$$\frac{i_j}{AnF} = \frac{\phi_j^z a_j}{A} = \frac{\phi_j^z (2j - 1)}{n_r^2} \tag{19}$$

The summation of all fractional fluxes, including the radial component, gives the total flux "through" the disk:

$$\frac{i}{AnF} = \Phi_{tot} = \sum_{j=1}^{n_r} \frac{\phi_j^z (2j - 1)}{n_r^2} + \frac{\phi_{n_r}^r (n_r - 0.5)}{2n_r^2} \tag{20}$$

If the calculation of the total current density takes into account only the normal flux perpendicular to the disk surface, the second term in eqn. (20) does not apply. An analysis of the fractional fluxes in the individual boxes shows that as the radial distance from the center increases, the increase in the amounts of the fluxes is initially almost linear, but in the vicinity of the electrode edge nonlinear. As a result the fractional currents in the outer range of the electrode are too small. This can be greatly improved by interpolating, with the aid of a smooth spline function, concentration values simulated at intervals of Δr, and recomputing the fractional fluxes in a suitably improved spatial network.

To ensure technical accuracy it is sufficient to subdivide the 3 outmost annular elements of the electrode in the ratio 1 : 10, and there to calculate the flux at 30 instead of 3 fixed points. The total flux, which includes only quantities in the normal direction to the electroactive surface, is given by the following function:

$$\frac{i}{AnF} = \Phi_{tot} = \sum_{j=1}^{n_r - 3} \frac{\phi_j^z (2j - 1)}{n_r^2} + \sum_{j=1}^{30} \frac{\phi_j'^z (n_r - 3.1 + 0.1j)}{5n_r^2} \tag{21}$$

The flux or current densities represented in eqns. (20) and (21) are the results of comprehensive model calculations This is best related to the real system by formulating both the experimental quantities, as well as the simulation parameters, as corresponding dimensionless expressions. Given this assumption, one obtains:

$$\chi \equiv \frac{\Phi_{tot}(l\ \Delta t)^{1/2}}{cD^{1/2}} = \frac{it^{1/2}}{nFAc^{b}D^{1/2}} \tag{22}$$

In accordance with this and Eqn. (8), the simulated Cottrell equation is

$$\chi = \pi^{-1/2}(1 + b\eta) \tag{23}$$

RESULTS AND DISCUSSION

The model computations were carried out for a large number of different parameter combinations. To facilitate a uniform evaluation and comparison with experimental values, all results were rendered in dimensionless form of eqn. (23) and listed as a function of $\eta \equiv (Dl\ \Delta t)^{1/2}/n_r\ \Delta r$ (Table 1).

Although there is not any known exact solution to the problem, the consistency (i.e. the right approximation of the differential equation studied) and accuracy of the numerical formulation can be easily verified. The value of the function of the modified Cottrell equation (1) converges to $\pi^{-1/2} = 0.56418\ldots$ where $t \to 0$, independent of the size of the factor b in the correction term. Therefore, the simulation must tend towards the same limit when its algorithms reflect a diffusion process at a planar disk electrode. On account of the initial discontinuity of the method, it is not possible to calculate exactly the mass flux for very small time values; hence, one determines its limiting behaviour indirectly from the slope of the current function. Under the reliable assumption that the slope of the latter is almost linear in the range $0 \leqslant \eta \leqslant 0.005$, one obtains the following limit condition which is "correct" in numerical and physical terms:

$$\lim_{t \to 0} \frac{\Delta\chi}{\Delta\eta} \equiv \mu = b\pi^{-1/2} \tag{24}$$

If the difference quotient μ assumes values $< b/\pi^{1/2}$ where time t is decreasing, the calculated current densities will be larger than theoretically desirable; vice versa, if $\mu > b/\pi^{1/2}$ they will be too small. In general, deviations in the limiting value up to 2% can be ascribed to reduced accuracy in computation owing to the mesh size of the grid. Larger differences would indicate an error in the principles underlying the model conception.

The estimates of the limiting values reveal a slight overvaluation of the radial diffusion in the boxes of the non-electroactive surface outside the disk ($k = 0$, $j > n_r$); hence, this simulation type always converges towards the exact current function from above [24]. If the radial component in layer 0 is eliminated, then, in keeping with expectations, the total flux across the disk surface will be too low. However, using a finer grid network both formulations converge towards a common function which completely satisfies eqn. (24). This fully confirms the consistency of the proposed model from the theoretical viewpoint.

TABLE 1

Simulated current function for diffusion-controlled current at finite disk electrodes: $\chi = \pi^{-1/2}\ (1 + b\eta)$. χ is the computed dimensionless representation of $it^{1/2}/nFAc^{b}D^{1/2}$, η corresponds to $(Dt/R^2)^{1/2}$; b is the variable coefficient of the correction term η

η	χ	b	η	χ	b	η	χ	b
0.002	0.5661	1.772	0.115	0.6828	1.83	0.40	1.0029	1.93
0.003	0.5672	1.774	0.120	0.6881	1.83	0.45	1.0621	1.96
0.004	0.5682	1.775	0.125	0.6935	1.83	0.50	1.1219	1.98
0.005	0.5692	1.776	0.130	0.6988	1.84	0.55	1.1822	1.99
0.006	0.5702	1.78	0.135	0.7042	1.84	0.60	1.2430	2.01
0.007	0.5712	1.78	0.140	0.7096	1.84	0.65	1.3042	2.02
0.008	0.5722	1.78	0.145	0.7150	1.84	0.70	1.3658	2.03
0.009	0.5732	1.78	0.150	0.7204	1.84	0.75	1.4277	2.04
0.010	0.5742	1.78	0.155	0.7258	1.85	0.80	1.4898	2.05
0.015	0.5793	1.78	0.160	0.7312	1.85	0.85	1.5521	2.06
0.020	0.5843	1.79	0.165	0.7367	1.85	0.90	1.6146	2.07
0.025	0.5894	1.79	0.170	0.7421	1.85	0.95	1.6773	2.08
0.030	0.5945	1.79	0.175	0.7476	1.86	1.00	1.7400	2.08
0.035	0.5996	1.79	0.180	0.7530	1.86	1.10	1.8658	2.10
0.040	0.6047	1.80	0.185	0.7585	1.86	1.20	1.9918	2.11
0.045	0.6098	1.80	0.190	0.7640	1.86	1.30	2.1181	2.12
0.050	0.6150	1.80	0.195	0.7695	1.87	1.40	2.2446	2.13
0.055	0.6202	1.80	0.200	0.7750	1.87	1.50	2.3713	2.14
0.060	0.6253	1.81	0.210	0.7861	1.87	1.60	2.4978	2.14
0.065	0.6305	1.81	0.220	0.7971	1.88	1.70	2.6245	2.15
0.070	0.6357	1.81	0.230	0.8083	1.88	1.80	2.7513	2.15
0.075	0.6409	1.81	0.240	0.8194	1.88	1.90	2.8780	2.16
0.080	0.6461	1.82	0.250	0.8306	1.89	2.00	3.0050	2.16
0.085	0.6514	1.82	0.260	0.8418	1.89			
0.090	0.6565	1.82	0.270	0.8531	1.90	3.00	4.2738	2.19
0.095	0.6616	1.82	0.280	0.8644	1.90	4.00	5.5461	2.21
0.100	0.6668	1.82	0.290	0.8758	1.90	5.00	6.8217	2.22
0.105	0.6721	1.83	0.300	0.8871	1.91	∞	—	2.2567
0.110	0.6774	1.83	0.350	0.9446	1.93			

Numerical calculations were made in addition for the mathematically simpler case of an infinite planar disk electrode. The convergence after only a few Δt loops was excellent, with an average error of 0.001% as compared to the analytical solution. That computational errors (truncation, discretization and round-off) have little influence upon the numerical accuracy is thus established beyond question.

Experimental chronoamperograms obtained at small disk electrodes [15] show that the numerical computations are in very good accordance with the experiment (Fig. 2). The deviation between experimental and theoretical data in the domain up to $\eta \leqslant 0.3$ is $<1\%$.

A comparison with the analytical solution derived by Aoki and Osteryoung [14] indicates that the simulation model fulfils very accurately their limiting conditions for $\eta \to 0$ and $\eta \to \infty$ (Fig. 2). In these cases the slope of our function corresponds to the predicted values of 1.772 . . . and 2.257 . . .. In Fig. 3 the slope values of the simulated current function are plotted against the dimension-

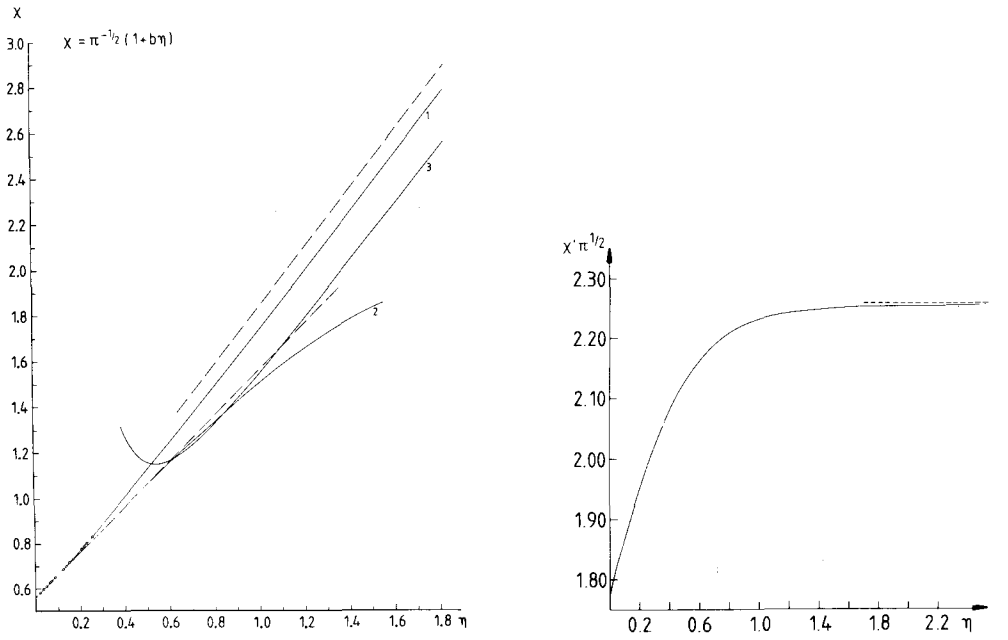

Fig. 2. Plot of experimental and computed $it^{1/2}$ data in the case of chronoamperometry with finite disk electrodes: (1) digital simulation — this work; (2, 3) curves by Aoki and Osteryoung [14] (asymptotic expansion and descending series); (- - - - - -) theoretically predicted slopes for $\eta \to 0$ and $\eta \to \infty$ [10, 14]; (· · · · · ·) experimental results [15].

Fig. 3. First derivative of the function $\chi = \pi^{-1/2}(1 + b\eta)$. The diagram shows the varying slope of the function χ in dependence on η; (- - - - - -) slope value for $\eta \to \infty$.

less parameter η. One observes that its monotonic change beginning at 1.772 is mainly restricted to the domain $0 < \eta < 1.0$. Above 1.0 the function approaches the constant slope of 2.26. An analysis of the calculated concentration profiles reveals that for $\eta > 0.6$ the radial concentration gradient reaches the center of the electrode. Consequently, concerning the flux through the electrode, a quasi-stationary situation gradually develops which, for values $\eta >> 1.0$, leads to a steady-state term for the current at the disk electrode. In contrast to our results, the slope in the i—t curve of Aoki and Osteryoung (small values of t, curve 2 in Fig. 2) at first decreases slowly. Therefore, close agreement with our model, i.e. a maximum difference of 1%, is only given up to $\eta \leqslant 0.2$. The medium part of the analytical function clearly deviates from our simulation; only in the long-time approximation ($\eta >> 2$) do the solutions approach each other again. Typical truncation errors which often influence the accuracy of explicit difference methods could be minimized by the use of an implicit technique. Thus, the model developed in this study should also possess a high degree of reliability for medium and large values of η. The results in the explicit solution of Sato et al. [13] are, in principle, similar to ours. However, the fractional fluxes in the outer elements of the electrode are slightly underestimated. For this reason the values of the explicit model are a little too low.

The concave curvature of the simulated i—$t^{1/2}$ function offers new insight

into non-linear effects always observed in chronoamperometric long time measurements at the disk electrode. Previous experimental findings present an unclear picture, as deviations from the linear shape of i—$t^{1/2}$ curves seem to appear irregularly and without any recognizable system. All attempts to explain this [1,8,9] accept the plausible hypothesis that these phenomena are due to convection influences, although similar effects at shielded electrodes have been registered remarkably seldom [5]. Comparing the model calculations and the experimental results [9,12,15—18] proves that a diffusion phenomenon is primarily responsible for the non-linear properties of the current function. Naturally, the diffusion model does not exclude the possibility that in actual experiments the mass transport to a stationary electrode can, in addition, simultaneously take place by convection. The probability of this is particularly high when measuring times exceed several minutes.

Surprisingly, one must deduce from the experimental and numerical results that the mass flux at the surface of a finite disk electrode deviates more strongly from the limiting conditions of the ideal linear diffusion than in the case of comparable spherical or cylindrical electrodes. For a long time the influence of the radial diffusion on planar electrodes was underestimated; for, in most earlier experiments, electrodes with a large area were normally used, which minimized the effect of the radial correction. The changes of several orders of magnitude which result from a decrease in the electrode surface are illustrated in Fig. 4. The radial current corrections i_{corr} in relation to the corresponding values of the linear diffusion i_{pl} are plotted against time for three representative electrode radii r_0 = 0.01, 0.001 and 1×10^{-4} m. The deviations from the ideal values are lowest for r_0 = 0.01 m; they reach the 1% mark only after an electrolysis time of 1 s. However, in the case of microelectrodes ($r_0 = 1 \times 10^{-4}$ m), whose surface size is much the same as fast dropping mercury electrodes, the 1% mark is reached well under 1 ms; here, for times above 1 s the corrective term is larger than the unaffected linear quantity. Recently, disk electrodes with small surfaces have become increasingly popular in experiments; this implies that data interpreted without taking radial diffusion into account contain considerable errors.

The picture of radial diffusion towards a circular plane would be incomplete without a description of the concentration distributions caused by such diffusion. Figure 5 shows the particularly interesting dimensionless concentration profiles c/c^b for three different electrode sizes at intervals of 0.1 concentration units. To facilitate comparison, the ordinates were normalized to the thickness of the linear diffusion layer, and the intervals on the abscissa were related to the individual electrode radii. The diagram depicts the concentration distribution at one point in time, namely after 10 s of electrolysis, where the diffusion coefficient has a mean value of 10^{-9} m^2 s^{-1}. In the case of an electrode with the radius 1×10^{-2} m, the linear diffusion layer is by and large preserved. It truncates at the level of the electrode edge, a phenomenon which illustrates the small effect of the radial diffusion under these conditions. By contrast, in the case of an electrode with radius 1×10^{-3} m there is a clear distortion in the radial direction. Where the radius is 1×10^{-4} m the quantities of radial and linear diffusion are almost equivalent.

A practical consequence of the simulation results is a modified method for the absolute determination of diffusion coefficients at small disk electrodes

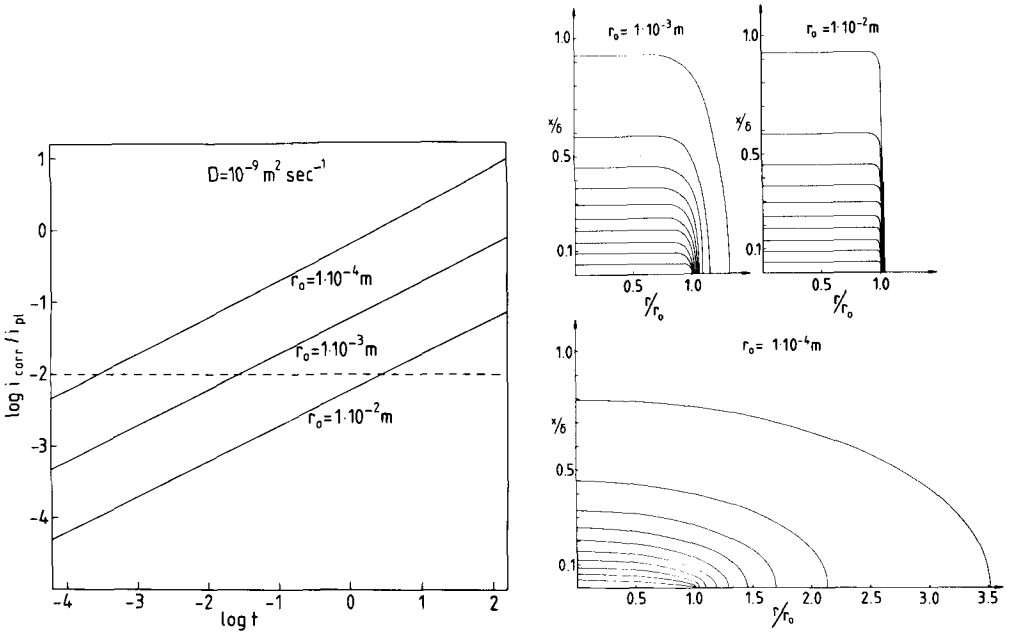

Fig. 4. Plot of log (i_{corr}/i_{pl}) vs. log t for a single potential-step experiment under diffusion control: (i_{corr}) radial current correction; (i_{pl}) current in the case of semi-infinite linear diffusion; (r_0) radius of disk electrode.

Fig. 5. Simulated concentration profiles at various finite disk electrodes (r_0 = 1 × 10^{-4}, 1 × 10^{-3}, 1 × 10^{-2} m) 10 s after start of electrolysis. Lines of equal fractional concentration are separated by 0.1 unit. Horizontal axis is r/r_0, the dimensionless distance across disk and insulator region. The vertical axis represents the distance perpendicular to the disk in relation to the thickness of the linear diffusion layer.

[13,15]. One advantage of this technique is reflected by the fact that the diffusion coefficient D and the charge transfer number n of an electroactive species could be determined simultaneously and accurately from a single "*it*" measurement. Furthermore, this model can successfully be used to analyze data obtained with micro disk electrodes, e.g. chrono- or potentiodynamic measurements in bioelectrochemistry. Knowledge of the working curve for diffusion-controlled current at micro disk electrodes facilitates the determination of concentrations in such systems, since no calibration procedures are needed. In addition, this simulation forms a basis for the quantitative description of edge effects in cyclic voltammetry and other transient techniques of electrochemistry. For this purpose only the initial and boundary conditions must be changed. Full details can be obtained on request from the author.

ACKNOWLEDGEMENT

The work was kindly supported by the Deutsche Forschungsgemeinschaft.

REFERENCES

1 R.N. Adams, Electrochemistry at Solid Electrodes, Marcel Dekker, New York, 1969.
2 P. Delahay, New Instrumental Methods in Electrochemistry, Interscience, New York, 1954.
3 F.G. Cottrell, Z. Phys. Chem., 42 (1902) 385.
4 H.A. Laitinen and I.M. Kolthoff, J. Am. Chem. Soc., 61 (1939) 3344.
5 M. von Stackelberg, M. Pilgram and V. Toome, Z. Elektrochem., 57 (1953) 342.
6 J. Zimmermann, Ph.D. Thesis, University of Kansas, 1964.
7 R. Lines and V.D. Parker, Acta Chem. Scand., B31 (1977) 369.
8 A.J. Bard, Anal. Chem., 33 (1962) 11.
9 P.J. Lingane, Anal. Chem., 36 (1964) 1723.
10 Z.G. Soos and P.J. Lingane, J. Phys. Chem., 68 (1964) 3821.
11 J.B. Flanagan and L. Marcoux, J. Phys. Chem., 77 (1973) 1051.
12 M. Kakihana, H. Ikeuchi, K. Tokuda and G.P. Sato, 25th Annual Meeting on Polarography and Electroanalytical Chemistry, 5th—6th Oct. 1979, Kobe.
13 M. Kakihana, H. Ikeuchi, G.P. Sato and K. Tokuda, J. Electroanal. Chem., 108 (1980) 381.
14 K. Aoki and J. Osteryoung, J. Electroanal. Chem., 122 (1981) 19.
15 J. Heinze, Ber. Bunsenges. Phys. Chem., 84 (1980) 785.
16 C.R. Ito, S. Asakura and K. Nobe, J. Electrochem. Soc., 119 (1972) 698.
17 M.A. Dayton, J.C. Brown, K.J. Stutts and R.M. Wightman, Anal. Chem., 52 (1980) 946.
18 K. Aoki and J. Osteryoung, J. Electroanal. Chem., in press.
19 S. Feldberg in A.J. Bard (Ed.), Electroanalytical Chemistry, Vol. 2, Marcel Dekker, New York, 1969, p. 199.
20 S. Feldberg in Computers in Chemistry and Instrumentation, Marcel Dekker, New York, 1972, p. 185.
21 J. Crank and P. Nicolson, Proc. Camb. Phil. Soc., 43 (1947) 50.
22 W.F. Ames, Numerical Methods for Partial Differential Equations, Academic Press, New York and San Francisco, 2nd edn., 1977.
23 D.W. Peaceman and H.H. Rachford, Jr., J. Soc. Ind. Appl. Math., 3 (1955) 28.
24 J. Heinze, unpublished results.
25 J. Douglas, Jr., J.A.C.M., 6 (1959) 48.